Regular Article

PHYSICAL CHEMISTRY RESEARCH
Published by the
Iranian Chemical Society
www.physchemres.org
info@physchemres.org

***Phys. Chem. Res.**, Vol. 6, No. 1, 67-82, March 2018*
DOI: 10.22036/pcr.2017.94247.1404

Interactions of Deferasirox as a Chelating Agent with Al and Ga Cations: A Theoretical Study on the $[M(DFX)_2]^{3-}$ Nanostructures

S. Salehi, M. Izadyar* and A.S. Saljooghi
Department of Chemistry, Faculty of Science, Ferdowsi University of Mashhad, Mashhad, Iran
(Received 1 August 2017, Accepted 13 October 2017)

A theoretical study was performed to evaluate the defersirox potency to chelate aluminum (Al) and gallium (Ga) as the toxic metals in biological systems. Deferasirox as an important class of chelators, which binds to the metallic center with the ratio of 1:2, is used to remove the toxic metals in the case of iron overload disease. The effects of water and DMSO as the solvent on the electronic nanostructures of $[Al(DFX)_2]^{3-}$ and $[Ga(DFX)_2]^{3-}$ were investigated by using the density functional theory and compared with the gas phase results. Natural bond orbital and quantum theory of atoms in molecules analyses was carried out to understand the nature of the complex bond character in the complexes. Topological analysis verified that deferasirox-aluminum complex is more stable than gallium complex, which is in good agreement with the experimental data. Natural charge analysis revealed that aluminum has a more positive character in comparison to gallium, therefore electron-donor atoms of the deferasirox bind to aluminum more favorable than gallium. TD-DFT studies showed a blue shift in the absorption spectra for the complexes in the presence of solvent. Based on different analyses, deferasirox is considered as a good chelator to remove aluminum and gallium cations in the biological systems.

Keywords: Deferasirox, Aluminum, Time-dependent DFT, Gallium, Solvent effect

INTRODUCTION

Ions are indispensable for life and some of the essential nutrients are in fact metal ions [1]. Many aspects of the interactions between the ions and living things are unknown, albeit it is possible to use spectroscopic measurements to gain knowledge on the structures of the ion-protein complexes. It has been revealed that the smaller size of metallic center makes it difficult to follow the binding process in the biological systems. [2].

Generally, drug molecules need to pass the lipid bilayer membrane barrier to reach their molecular targets [3]. Computational studies could be a powerful tool to make a comprehensive understanding about such cellular transportation kinetics and thermodynamic mechanism that are, in turn, key factors in understanding and prediction of the bioavailability of the drugs. Knowing these promenant factors will have an important role in the development of new drugs as well as drug delivery processes. [4,5].

The term of chelation therapy is used in Fe-overload diseases to reduce the toxic effects of the excess iron in the cells [6]. The first class of the iron chelators, desferrioxamine (DFO), was introduced in 1960 [7]. The development of new classes of the iron chelators is as an inevitable part of the pharmaceutical chemistry. Previously reported iron chelators such as DFO has a lot of drawbacks such as short half-life, cost efficiency and side effects which limit their applications [8]. The hard nature of Iron(III) caused to scientists design many of these chelators in the way that the oxygen atom be a part of donor groups such as polyaminocarboxylic acids (EDTA, DTPA), catechols, or deferasirox [9].

Deferasirox (4-[3,5-bis(2-hydroxyphenyl)-1,2,4-triazol-1yl]-benzoic acid, or ICL670) was first reported in 1999 [10]. Deferasirox has a high tendency for binding to Fe^{3+},

*Corresponding author. E-mail: izadyar@um.ac.ir

and its NO_2 donation arises from one triazole nitrogen and two phenolate oxygen donors. A high affinity of DFX to bind to trivalent Fe^{3+} and a little affinity for other divalent ions such as Zn^{2+} or Cu^{2+} makes it an ideal chelator in iron overload disease [11]. Firstly, deferasirox was approved by FDA as an oral chelator in 2005, in the treatment of disease related to the iron overload such as Parkinson's [12,13]. The aromatic rings in the structure of DFX improved the infusion of deferasirox in the biological membranes; the chelate formation of the deferasirox with iron within the cells have been proved by *in vitro* and *in vivo* studies [14]. In vitro, chelation potential of deferasirox in removal of the different toxic metal ions such as Hg, Tl, Cd and V has been investigated, recently [15].

The complexation modes of iron chelators with other metallic center such as Ga(III) and Al(III) are often investigated instead of Fe(III) by NMR [16]. A reasonable correlation between the Alzheimer's disease (AD) and aluminum was proved, previously [17,18]. Also, the aluminum accumulation in the NFT-bearing neurons was verified by X-ray spectrometric method in 1980 [19]. Laser microprobe techniques confirmed that the amount of aluminum increases within AD neurons [20]. Meanwhile, gallium usage has gained an importance in the fields of medicinal chemistry and electronic devices. The radioactive gallium and stable gallium nitrate are used as powerful diagnostic and therapeutic compound in medicine [21]. Therefore, the remaining of the Al or Ga ions in the body for a long time would be the origin of some diseases. As a consequence, finding an appropriate chelator to excrete these toxic metals seems to be vital.

The equilibrium constants of the deferasirox-iron chelated form have been investigated, theoretically [22,23]. In the present study, the chelation potency of deferasirox as an important class of chelators in Al and Ga removal is investigated. Thermodynamic constants of the nano-complexes of $[Al(DFX)_2]^{3-}$ and $[Ga(DFX)_2]^{3-}$ in the gas, water and DMSO are calculated. The chemical specificity of these complexes, bond characters and electronic transitions are carried out, using the NBO (Natural Bond Orbital) and QTAIM (quantum theory of atoms in molecules) analyses. The M-L bonds properties of the deferasirox-metal complexes $[M(DFX)_2]^{3-}$, M (M = Al, Ga), *via* electron localization function (ELF) and localized orbital locator (LOL) are considered as well. To do so, ELF and LOL are computed using the Multiwfn 3.3.6 [24] software. Additionally, the absorption spectrum is predicted by time-dependant density functional theory (TD-DFT).

COMPUTATIONAL DETAILS

Geometry optimization was carried out with the hybrid exchange-correlation functional B3LYP along with the relativistic basis set of Lanl2dz for metal ions and 6-311 G(d,p) for non-metal atoms, using the default convergence criterion [25]. Frequency calculations were carried out in order to estimate the zero-point vibrational energies (ZPVEs), for all structures in the gas phase and solvents and confirmation of the stability of the structures with the real frequencies. Stability constants were calculated at 298.15 K according to the experimental conditions.

The accuracy of DFT methods in inorganic and organometallic systems makes them powerful tools in theoretical calculations. Their ability to calculate a wide range of molecular properties makes a strong connection between the results of experimental and theoretical studies. The results obtained from the DFT methods often provide important information about the geometric, electronic, and spectroscopic properties of the studied systems [26,27].

The solvent (water and DMSO) effects on the binding process of deferasirox to the cationic centers (Al(III) and Ga(III)) were investigated. To do so, the conductor like polarizable continuum model (CPCM) was applied. Natural bond orbital analysis, introduced by Reed [28], was carried out at the B3LYP/6-311G(d,p) level to explore the distribution of electrons into atomic and molecular orbitals and contributions of the covalent bonding to the high chemical specificity of the $[M(DFX)_2]^{3-}$ complexes [29]. Based on this analysis, donor-acceptor interactions for the reactants and final products were fully evaluated. Quantum chemistry reactivity indices of the isolated compounds were determined in order to describe the reactivity trend of the studied compounds. Topological properties were analyzed by using the Bader's theory of atoms in molecules in AIM2000 package, using the wave functions generated from the B3LYP/6-311G(d,p) results [30]. To obtain further evidences about the new bonds nature of the complexes between M (M = Al, Ga) and deferasirox molecule, some

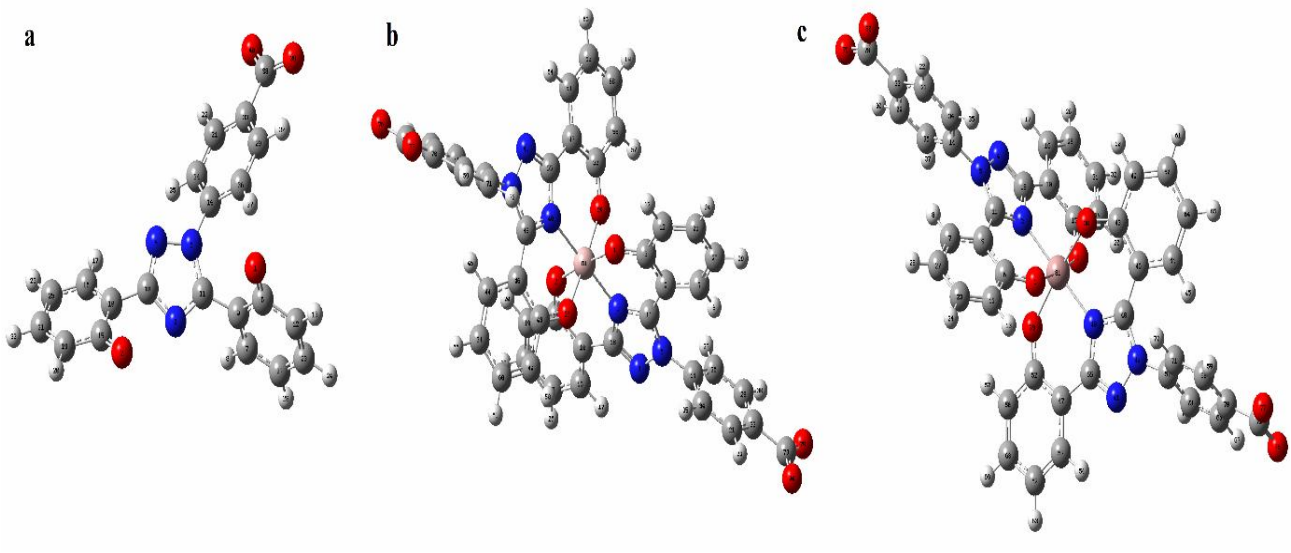

Fig. 1. Optimized structures of (a) deferasirox, (b) $[Al(DFX)_2]^{3-}$, and (c) $[Ga(DFX)_2]^{3-}$.

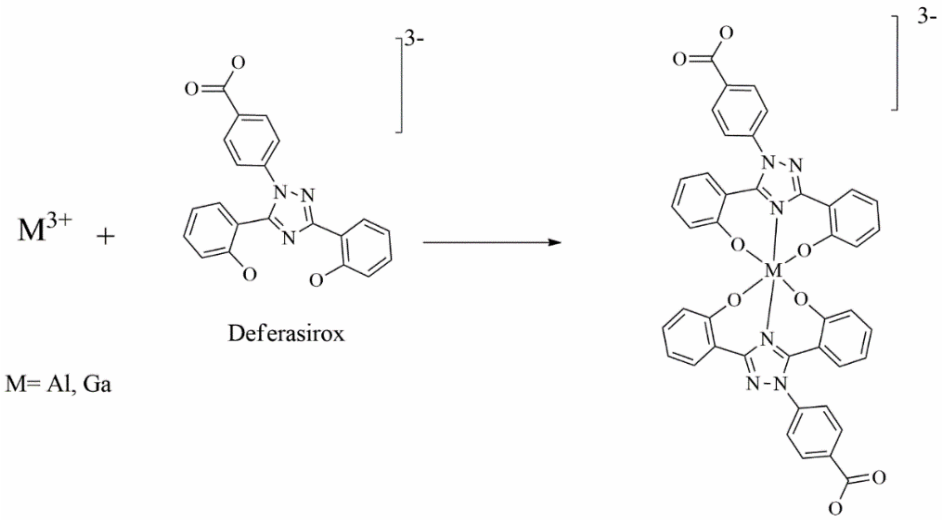

Scheme 1. Chelation process of deferasirox and metal center

extensively used analysis techniques such as the LOL and ELF have also been carried out. Additionally, TD-DFT method was applied to investigate the electronic transition property due to its effect in the prediction of electronic and also optical properties of inorganic and organic complex molecules [31].

RESULTS AND DISCUSSION

Local Bonding Structure and Equilibrium Constant

The stable optimized molecular structures of the complexes are shown in Fig. 1. Selected bond lengths and bond angles of the compounds are listed in Table S1. The

calculated results indicated that in all cases, the M-N bonds, having N atoms with sp^2 hybridation, are longer than M-O ones in which the solvent has no important effect on the bond length. Specifically, d_{M-N}, and d_{M-O} for gallium complexes are greater than that of the aluminum complex, which arises from the increasing metal atomic radius of $r_{Al} < r_{Ga.}$. Moreover, the angles of N3-M-O1-O2 and N40-M-O38-O39 are about 90° and O1-M-O2, O38-M-O39 and N3-M-N40 angles are close to 180° in the obtained complexes indicating that these complexes get an octahedral structure.

The preference of the deferasirox to chelate with small metal cation is due to the rigid structure of two six-membered chelate rings. This property is of importance regarding the selectivity of this ligand in the biological systems [23]. The formation of the metal complexes (Al, Ga) and deferasirox was investigated and the results of the equilibria are summarized in Table 1. Scheme 1 shows the optimized chemical structure of the $[M(DFX)_2]^{3-}$ complex.

Based on Table 1, deferasirox shows more tendency to chelate aluminum rather than gallium. The solvent has a different influence on the equilibrium constants of two complexes. In Al complexes, these equilibrium constants decrease in the presence of solvent which is in contrast to Ga complexes. The highest value of the equilibrium constant belongs to $[Al(DFX)_2]^{3-}$ complexes in the gas phase. It is suggested that unpredictable high stability constant of the Al(III) complex is due to steric factors. The inflexible orientation of the donor sets having an ideal preorientation, along with the fact that six-membered chelate rings are exclusively formed, obviously favor complex formation with small Al(III) cation. This condition is not applicable in the case of Ga(III) complex, because of high radius of gallium, although the equilibrium constant of the gallium complex is considerable.

IR Spectrum

The IR spectrum of the $[Al(DFX)_2]^{3-}$ and $[Ga(DFX)_2]^{3-}$ complexes are illustrated in Fig. 2. The spectrums showed three sharp peaks at 1714.62 cm^{-1}, 1508 cm^{-1} and 1338 cm^{-1} which are assigned to the C=O asymmetric stretching bond, C-H stretching and C=O bending vibration, respectively. Selected vibrational frequencies of the optimized complexes are summarized in Table 2. From the table, it can be concluded that solvent causes a slight decrease in the C=O stretching frequency, while this value is constant in the water and DMSO in both complexes.

The M-O bond frequency has a greater value in the gas phase, which is smaller for the gallium complexes. The frequency of the M-N bonds in the aluminum complexes are greater than that of the gallium complexes, however both complexes show a similar behavior in the presence of the solvents.

Electron Localization Function and Localized Orbital Locator

The ELF and LOL analyses were employed for quantitative and qualitative explanation of the M-L bonds in the complexes. ELF offers access to chemically intuitive domains beyond the atomic centers encompassing bonds and lone pairs. The ELF values are in the range of 0-1. The perfect electron localization corresponds to 1 value for ELF [32]. LOL indicates the location and characterization bond effects in relations to the kinetic energy contributions. High and low values of the LOL indicate the slow and fast electrons, respectively, which the slow electrons are localized electrons such as in bond or lone pair. Consequently, a larger value of the ELF and LOL is correlated with a higher electron density [33].

Figure 3 shows the ELF, LOL and the electron density at the center of the studied complexes. On the basis of the ELF and LOL maps, there is a medium electron density localized between the M and L, clearly revealing that the M and L bonding interaction has a partial covalent bond character. However, in the case of the gallium complexes, higher values of the ELF between the M and L centers indicates an increase in the electron density localization, supporting a slightly stronger covalent bond character. According to Fig. 3, it is obvious that the solvent slightly changes the electron density which in turn alters the bond characteristics.

Absorption Spectrum

The electronic spectra of the $[Al(DFX)_2]^{3-}$ and $[Ga(DFX)_2]^{3-}$ complexes were calculated by the TD-DFT method at the B3LYP/6-311G(d,p) level. The TD-DFT principal electronic transitions, excitation energies and oscillator strengths are summarized in Table 3, together

Table 1. Calculated Equilibrium Constants for M(III)-deferasirox Complexes (M = Al, Ga)

logK	Gas	Water	DMSO
$[Al(DFX)_2]^{3-}$	1145.19	935.40	937.83
$[Ga(DFX)_2]^{3-}$	174.93	399.91	398.52

Table 2. Selected Vibrational Frequencies in the IR Spectrum of $[Al(DFX)_2]^{3-}$ and $[Ga(DFX)_2]^{3-}$ Complexes (cm^{-1})

	$[Al(DFX)_2]^{3-}$			$[Ga(DFX)_2]^{3-}$		
	Gas	Water	DMSO	Gas	Water	DMSO
ν(C=O)	1714.62 [a]	1669.65	5416.69	1714.32	1669.35	1669.59
	1338.98 [b]	1362.98	1362.47	1338.89	1360.22	1360.25
ν(C-H)	1508.24	1505.30	1505.22	1503.25	1500.25	1500.65
ν(M-O)	358.89	860.34	860.29	870.95	865.24	865.32
ν(M-N)	1020.00	1013.25	1013.25	1016.35	1010.56	1010.35

[a]C=O bond asymmetric stretching mode frequency. [b]C=O bond asymmetric bending mode frequency.

with the major one-electron transitions contributing to the excited-state of complexes. Figure 4 represents the absorption spectra of the $[Al(DFX)_2]^{3-}$ and $[Ga(DFX)_2]^{3-}$ complexes in the gas phase, water and DMSO. On the basis of Fig. 4, the absorption spectrum of $[Al(DFX)_2]^{3-}$ containing two distinguish absorption bands at 381.3 nm (lower energy) and 337.5 nm (higher energy) peaks. The low-energy electronic transition was assigned by a more contribution of the HOMO→LUMO excitations and less contribution of the H-1→L+1 transition. The HOMO is delocalized on the Al and DFX, while the LUMO is mainly located on the DFX, indicating obvious charge transfer (CT). The peak observed at 337.5 nm is associated with the H-9→LUMO, H-2→L+2, HOMO→L+2 transitions. In the case of the H-2→L+2 transition, the electron density of the H-2 part is mainly located around the metallic center, while in the L+2 state, electron density is contributed on the ligand atoms.

These differences between the electron densities can be interpreted as the charge transfer from the metal to the ligand orbitals (MLCT). Moreover, solvent considerably affects the adsorption spectrum of the aluminum complex. On the basis of Table 3 and Fig. 4, the sharpness of λ_{max} increases in water, due to the net charge transfer from HOMO→LUMO, whereas the higher energy peak has a lower intensity in comparison to the gas phase.

A significant change in the UV spectrum is observed by replacement of M in $[Al(DFX)_2]^{3-}$ by Ga in the gas phase. Higher energy peaks in the aluminum complex spectrum is diminished, while a sharp peak is observed in the gallium complex. In the gas phase spectrum of gallium, λ_{max} appeared in 408 nm. In the spectrum of the gallium complex, the sharp peak mainly arises from a charge transfer of HOMO→LUMO and H-1→L+1. Similar to

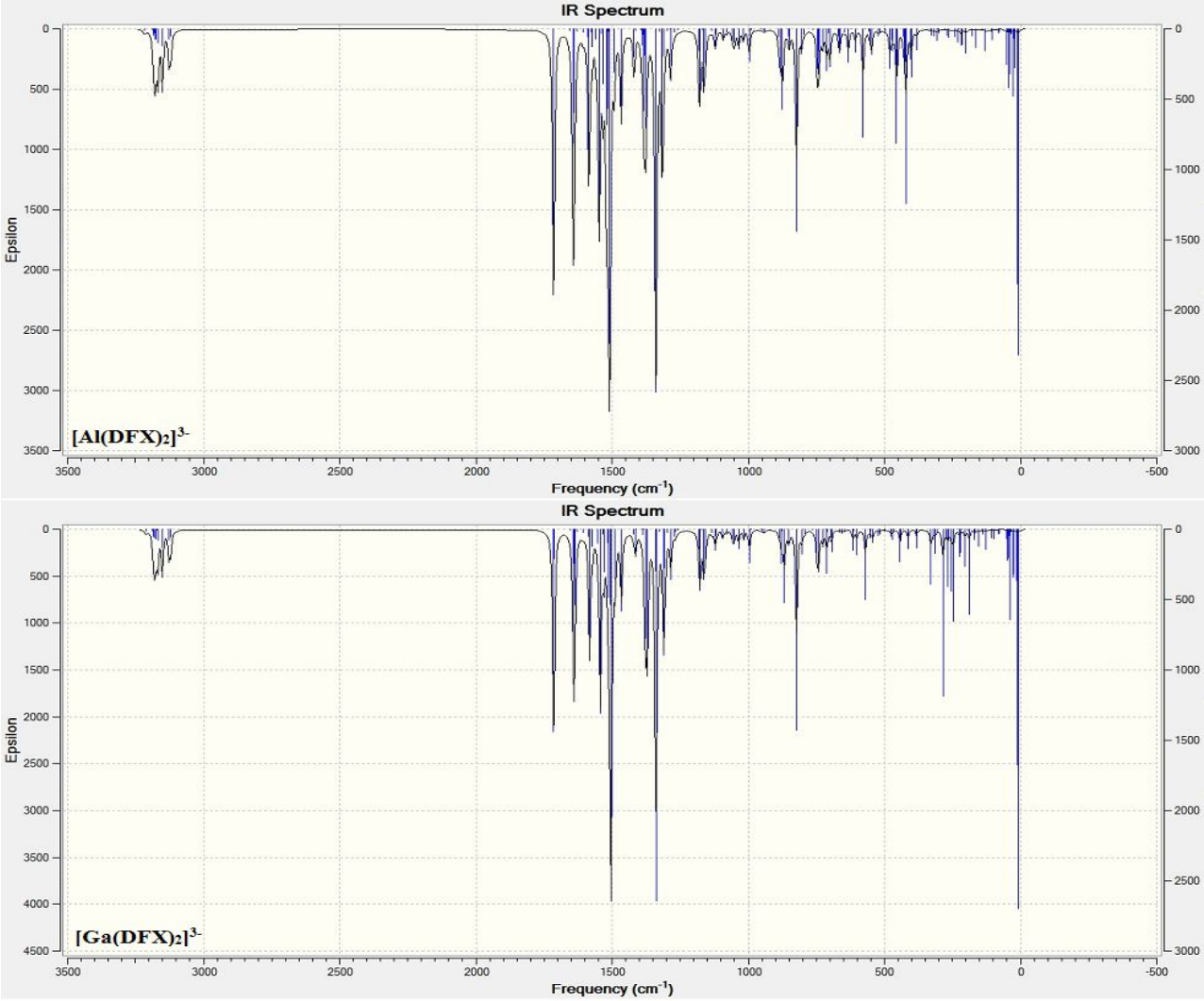

Fig. 2. IR spectrum of $[Al(DFX)_2]^{3-}$ and $[Ga(DFX)_2]^{3-}$ complexes.

aluminum complex, HOMO is distributed on Ga and DFX, while LUMO is on the deferasirox part.

In the case of gallium complex in water, there are two peaks at 317.1 nm and 371 nm. The obtained λ_{max} is correlated with the charge transfer from HOMO→LUMO. The higher energy peak is assigned as delocalization of electron density from the H-3→L+1 and H-2→LUMO. Obviously, the absorption spectra in DMSO is nearly similar to water with a slight difference and the solvent induces a blue shift of 37 nm in the spectrum of the gallium complex. The results confirm that the absorption spectrum of $[Ga(DFX)_2]^{3-}$ complexes are more impressible in the presence of the solvent rather than aluminum analogous.

The molecular orbitals involved in the relatively intense electronic transitions in the absorption spectra of the $[Al(DFX)_2]^{3-}$ and $[Ga(DFX)_2]^{3-}$ complexes in the gas phase, water and DMSO are presented in Fig.5.

NBO Analysis

To calculate the bonding orbital with maximum density, NBO analysis is a powerful tool. In fact, the quantification of Mulliken charges, the occupancy of atomic orbitals, and

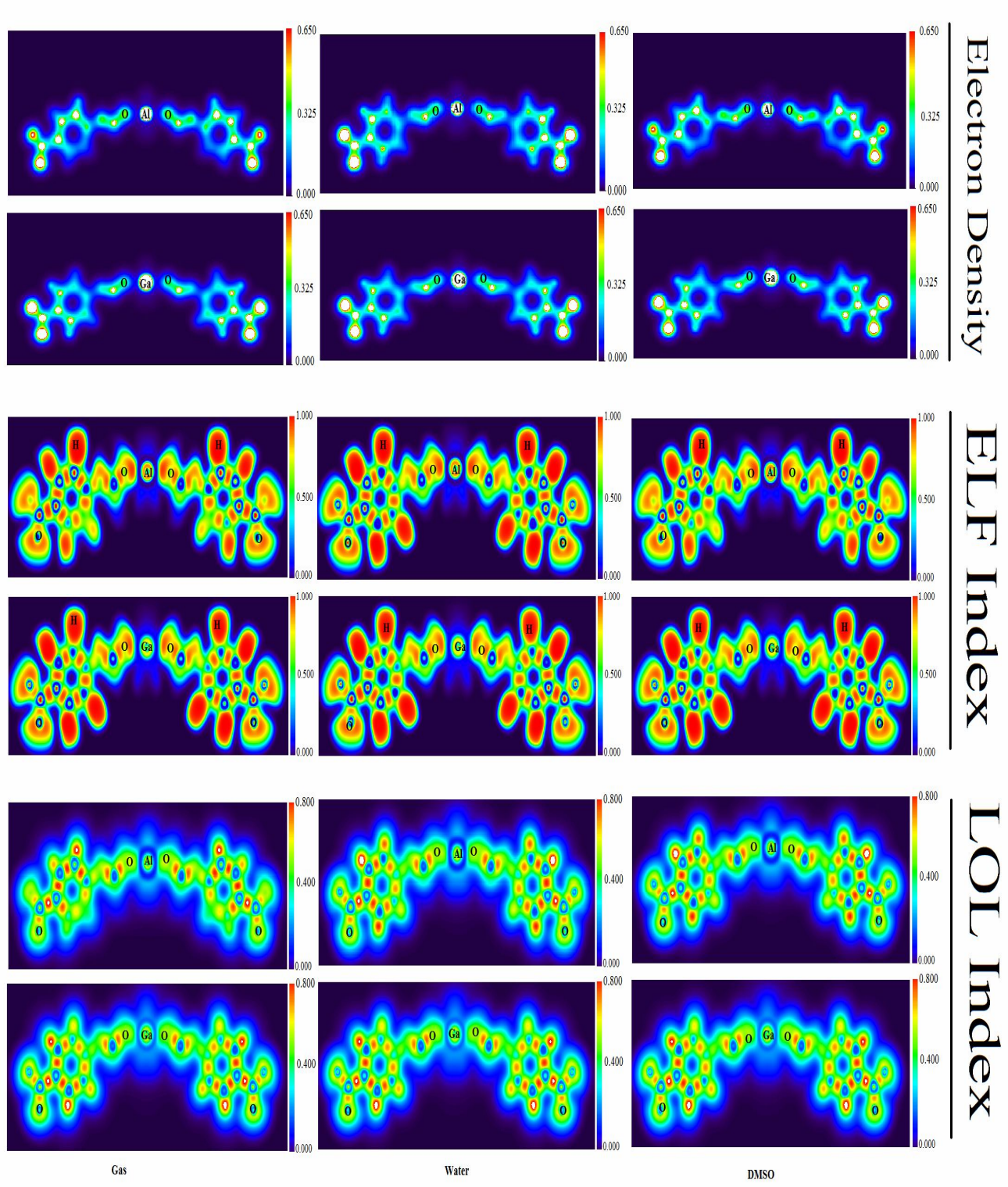

Fig. 3. Theoretical maps of the ELF, LOL and electron density of the $[Al(DFX)_2]^{3-}$ and $[Ga(DFX)_2]^{3-}$ complexes.

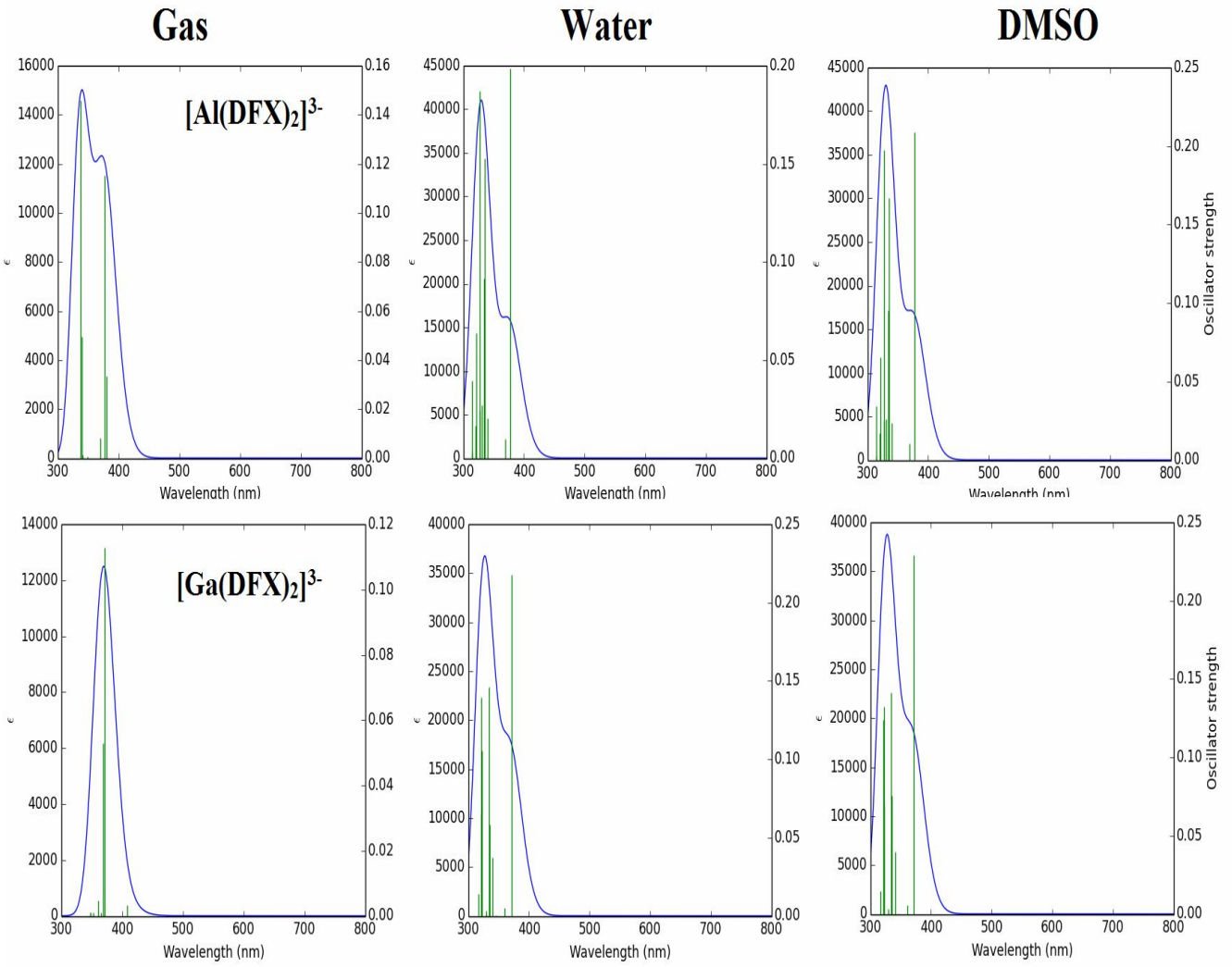

Fig. 4. Absorption spectra of the $[Al(DFX)_2]^{3-}$ and $[Ga(DFX)_2]^{3-}$ complexes calculated at the B3LYP/6-311G(d,p) level.

evaluation of atomic orbital contributions to the molecular orbitals are provided by NBO studies. The occupancy of the natural atomic orbitals agreed with the expected occupancy for the given nuclear charges and calculated electronic charges of the metals. Using the second-order perturbation theory analysis of the Fock matrix, donor-acceptor interactions were calculated for the complexes, and the stabilization energy E(2), from the donor to the acceptor orbitals were evaluated [34,35].

In order to investigate the stabilization energies of the metal complexes in the gas, water and DMSO, NBO analysis was carried out and the significant NBO interactions were reported in Table 4. Considering this table, it can be concluded that metal centers are electron acceptor and the coordinated atoms (O and N) transfer the electron density to the metal centers. In agreement with the experimental results [36], electron charge transition from N atom, in all cases has a lower intensity in comparison to O atoms. N atoms with sp^2 hybirdation would generate a high tendency to bind to the divalent biometalic cations, because sp^2 nitrogen atom is slightly softer than a negatively charged oxygen donor [37,38]. NBO analysis justifies why

Table 3. Simulated Wavelengths (nm), Energies (eV), Oscillator Strengths, and Major Contributions for $[Al(DFX)_2]^{3-}$ and $[Ga(DFX)_2]^{3-}$ Complexes Calculated at the B3LYP/6-311G(d,p) Level

Complex		Wavelength	Energy	Oscillator strength	Excitation (%composition)
$[Al(DFX)_2]^{3-}$	Gas	381	3.2516	0.0335	HOMO→LUMO (58%), H-1→L+1 (26%)
		337	3.6738	0.1457	H-2→L+2 (62%), HOMO→L+2 (17%), H-9→LUMO (11%)
	Water	377	3.2890	0.1984	HOMO→LUMO (98%)
		314	3.9460	0.0394	HOMO→L+4 (63%), H-4→LUMO (7%)
	DMSO	377	3.2859	0.2089	HOMO→LUMO (98%)
		314	3.9436	0.0341	HOMO→L+4 (53%), H-4→LUMO (11%)
$[Ga(DFX)_2]^{3-}$	Gas	408	3.0348	0.0033	HOMO→LUMO (54%), H-1→L+1 (30%)
	Water	371	3.3425	0.2175	HOMO->LUMO (98%)
		317	3.9112	0.0141	H-3→L+1 (90%), H-2→LUMO (6%)
	DMSO	371	3.3395	0.2291	HOMO→LUMO (97%)
		317	3.9103	0.0145	H-3→L+1 (90%), H-2→LUMO (6%)

Assignment: H = HOMO, L = LUMO, H-1 = HOMO-1, L + 1 = LUMO + 1, et.

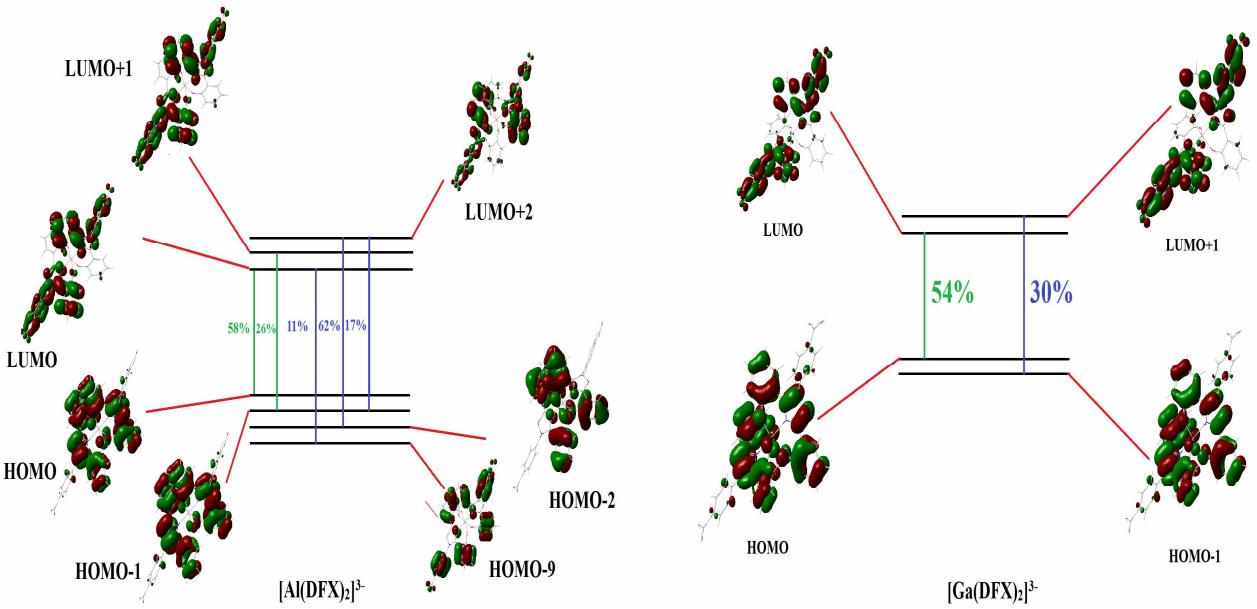

Fig. 5. The molecular orbitals involved in the relatively intense electronic transitions in the absorption spectra of the $[Al(DFX)_2]^{3-}$ and $[Ga(DFX)_2]^{3-}$ complexes in the gas phase.

Table 4. Significant Natural Bond Orbital Interactions of the $[M(DFX)_2]^{3-}$ (M = Al, Ga) Complexes and their Second Order Perturbation Stabilization Energies (kcal mol^{-1})

Complex	Natural Bond Orbital Interactions		E(2)		
	Donor	Acceptor	Gas phase	Water	DMSO
$[Al(DFX)_2]^{3-}$	LP_{O1}	LP^*_{Al}	19.1	19.7	19.6
	LP_{O2}	LP^*_{Al}	19.3	18.8	19.8
	LP_{N3}	LP^*_{Al}	64.4	64.4	64.2
	LP_{O38}	LP^*_{Al}	19.1	19.7	19.6
	LP_{O39}	LP^*_{Al}	19.3	19.8	19.8
	LP_{N40}	LP^*_{Al}	63.6	64.35	64.2
$[Ga(DFX)_2]^{3-}$	LP_{O1}	LP^*_{Ga}	21.2	21.7	21.7
	LP_{O2}	LP^*_{Ga}	22.1	23.0	22.9
	LP_{N3}	LP^*_{Ga}	77.2	78.4	78.4
	LP_{O38}	LP^*_{Ga}	21.2	21.7	21.7
	LPO_{39}	LP^*_{Ga}	22.1	23.0	22.9
	LP_{N40}	LP^*_{Ga}	77.2	78.4	78.4

Table 5. Electrostatic Charges of the Atoms at the Center of the Reaction for $[M(DFX)_2]^{3-}$ (M = Al, Ga) Complexes

Complex	Atom	Gas phase	Water	DMSO
$[Al(DFX)_2]^{3-}$	Al	1.80	1.82	1.82
	O1	-0.79	-0.83	-0.82
	O2	-0.80	-0.85	-0.85
	N3	-0.58	-0.62	-0.62
	O38	-0.79	-0.86	-0.82
	O39	-0.80	-0.85	-0.85
	N40	-0.58	-0.62	-0.62
$[Ga(DFX)_2]^{3-}$	Ga	1.70	1.64	1.63
	O1	-0.77	-0.80	-0.79
	O2	-0.80	-0.83	-0.83
	N3	-0.59	-0.59	-0.59
	O38	-0.76	-0.80	-0.79
	O39	-0.80	-0.83	-0.83
	N40	-0.59	-0.59	-0.59
Deferasirox	O2	-0.86	-0.94	-0.93
	O3	-0.82	-0.92	-0.92
	N4	-0.74	-0.89	-0.89

Table 6. Topological Properties and their Laplacian, $\nabla^2\rho$, (a.u.) for $[Al(DFX)_2]^{3-}$ and $[Ga(DFX)_2]^{3-}$ Obtained from AIM calculations

	$[Al(DFX)_2]^{3-}$								$[Ga(DFX)_2]^{3-}$									
	Gas			Water				DMSO	Gas			Water				DMSO		
	ρ	-V/G	$\nabla^2\rho$	ε	ρ	-V/G	$\nabla^2\rho$	ρ	-V/G	$\nabla^2\rho$	ρ	-V/G	$\nabla^2\rho$	ρ	-V/G	$\nabla^2\rho$	ρ	-V/G	$\nabla^2\rho$
M-O1	0.063	0.970	-0.107	0.091	0.062	0.974	-0.108	0.089	0.061	0.971	-0.108	0.079	1.170	-0.088	0.079	1.170	-0.088	0.079	1.170	-0.088
M-O2	0.064	0.971	-0.109	0.094	0.064	0.974	-0.103	0.093	0.064	0.974	-0.103	0.082	1.165	-0.082	0.082	1.165	-0.082	0.082	1.166	-0.082
M-N3	0.054	1.032	-0.072	0.073	0.056	1.032	-0.076	0.075	0.056	1.030	-0.076	0.079	1.271	-0.063	0.079	1.272	-0.063	0.080	1.272	-0.063
M-O38	0.063	0.970	-0.107	0.091	0.061	0.974	-0.108	0.089	0.061	0.974	-0.108	0.079	1.170	-0.088	0.079	1.170	-0.088	0.079	1.170	-0.088
M-O39	0.064	0.971	-0.109	0.094	0.064	0.974	-0.103	0.093	0.064	0.974	-0.103	0.082	1.165	-0.082	0.082	1.166	-0.082	0.082	1.166	-0.082
M-N40	0.054	1.032	-0.072	0.073	0.056	1.032	-0.076	0.075	0.056	1.032	-0.076	0.079	1.272	-0.063	0.080	1.272	-0.063	0.080	1.272	-0.063

equilibrium constants of the $[Al(DFX)_2]^{3-}$ are greater than $[Ga(DFX)_2]^{3-}$. Electron density transfers from the donor set ($LP_{O1,\ 38}$, $LP_{O2,\ 39}$ and $LP_{N3,\ 40}$) to LP^*_M in the aluminum complex are less than those in gallium because of a greater radius of gallium. Therefore, the interaction of gallium LP* orbitals and LP donor atoms are stronger. Also, it is clear that the solvent improves the electron transfer into the LP* orbital of the metal atom, which in turn, reduces the equilibrium constant.

Ligand to Metal Charge Transfer

Partial distribution of the atomic charges on the free ligand, $[Al(DFX)_2]^{3-}$ and $[Ga(DFX)_2]^{3-}$ complexes were calculated. Here, ChelpG charges were estimated at the B3LYP/6-311++G(d,p) level and the results are represented in Table 5.

According to Table 5, solvent molecules induce a negative charge on the donor atoms in comparison to the gas phase, consequently the electron density transfer to the metal LP* is simplified, which in turn elevates the stability of complexes in the gas phase. However, a more negative character of the atomic charge is followed by a stronger electrostatic interaction between the metal center and ligand, which is clear for the gallium complex. On the other hand, the positive charge on the metal center of the gallium complex is less than aluminum so the equilibrium constant for aluminum complex is higher. There are similar results for the stability of gallium complexes in different phases.

Topological Properties

Table 6 shows the electron density, ρ, the potential energy density to the kinetic energy density ratio, -V/G, and the laplacian property of the electron density, $\nabla^2\rho$ calculated by QTAIM method. The value of electron density at the bond critical point (BCP), ρ, is a measure of the bond strength [39]. A shared interaction (covalent bond) is characterized with $\rho > 0$ au and a negative value of the Laplacian at the BCP. Conversely, a closed shell interaction (ionic bond), is characterized by $\rho < 0$ au and a small positive value of the Laplacian. On the basis of the values reported in Table 5, $\rho > 0$ and $\nabla^2\rho < 0$, the covalence bond character for both complexes in the gas phase, water and DMSO are predicted. However the corresponding values for the gallium complexes represent a less covalent bond character [40].

Another reliable tool in QTAIM analysis is the potential energy density to kinetic energy density ratio, -V/G, that may be applied to determine the nature of a chemical bond. Ionic interactions and typically covalent interactions are determined by $-V/G \leq 0.5$ and $-V/G > 1$, respectively, and $0.5 < -V/G < 1$ is related to the intermediate characters or partial covalent bond [41]. Specially in the $[Al(DFX)_2]^{3-}$ complexes, the M-O bond showed a partial covalent bond character, while the M-N bond showed a covalence behavior. Whereas, in the case of the gallium complexes, all M-O and M-N bonds showed a covalence bond character. According to the obtained topological properties, gallium complexes has a more covalent character rather than Al, which arises from $r_{Al} < r_{Ga}$.

In order to investigate the π character of a bond, the ellipticity (ε) indexes in the QTAIM analysis were calculated. Equation (1) represents the ε definition, where λ1 and λ2 are the negative eigenvalues of the Hessian of the electron density at the BCP, according to the theoretical trend of: $\lambda1 < \lambda2 < 0 < \lambda3$. Because of the negative values of λ1 and λ2, ε always is a positive value [42].

$$\varepsilon = \lambda1\backslash\lambda2 - 1 \quad (1)$$

According to the obtained values for ε, gallium complexes have a greater ellipticity than aluminum, indicating an advanced π-bonding for gallium (Table 7).

DFT Reactivity Indices

Quantum chemistry reactivity indices were estimated according to the procedure proposed by Parr [43]. These parameters include the electronic chemical potential (μ), electronic chemical hardness (η) and the global electrophilicity index (ω). The last descriptor, ω, measures the stabilization in the energy when a system acquires an additional electronic charge from the environment. [44] Other DFT reactivity indices were calculated based on the frontier orbital energies and reported in Table 8.

A high chemical hardness is as a consequence of the large HOMO-LUMO gap that means a good structural stability. High stability, in turn, indicates low chemical

Table 7. The Ellipticity (ε) Values, Calculated by QTAIM Methods in the $[Al(DFX)_2]^{3-}$ and $[Ga(DFX)_2]^{3-}$ Complexes

$[Al(DFX)_2]^{3-}$												
	Gas				Water				DMSO			
Bond	λ1	λ2	λ3	ε	λ1	λ2	λ3	ε	λ1	λ2	λ3	ε
M-O1	-0.100	-0.097	0.627	0.091	-0.097	-0.093	0.602	0.089	-0.097	-0.093	0.602	0.089
M-O2	-0.103	-0.099	0.641	0.094	-0.102	-0.098	0.602	0.093	-0.102	-0.098	0.602	0.093
M-N3	-0.077	-0.074	0.441	0.073	-0.081	-0.078	0.465	0.075	-0.081	-0.078	0.465	0.075
M-O38	-0.100	-0.097	0.627	0.091	-0.097	-0.093	0.602	0.089	-0.097	-0.093	0.602	0.089
M-O39	-0.103	-0.099	0.641	0.094	-0.102	-0.099	0.632	0.093	0.102-	-0.099	0.632	0.093
M-N40	-0.077	-0.074	0.441	0.073	-0.081	-0.078	0.466	0.075	-0.081	-0.078	0.466	0.075
$[Ga(DFX)_2]^{3-}$												
M-O1	-0.106	-0.102	0.534	0.096	-0.106	-0.101	0.535	0.096	-0.106	-0.101	0.535	0.096
M-O2	-0.113	-0.108	0.573	0.102	-0.112	-0.108	0.573	0.101	-0.112	-0.108	0.573	0.101
M-N3	-0.103	-0.100	0.455	0.094	-0.103	-0.101	0.455	0.094	-0.103	-0.101	0.455	0.094
M-O38	-0.106	-0.102	0.534	0.096	-0.106	-0.101	0.535	0.096	-0.106	-0.101	0.535	0.096
M-O39	-0.113	-0.108	0.573	0.102	-0.112	-0.108	0.573	0.101	-0.112	-0.108	0.573	0.101
M-N40	-0.103	-0.100	0.455	0.094	-0.103	-0.101	0.455	0.094	-0.103	-0.101	0.455	0.094

Table 8. DFT Reactivity Indices for Deferasirox and $[M(DFX)_2]^{3-}$ (M = Al, Ga) Complexes (a.u.)

Compound	Gas phase			Water			DMSO		
	$-\mu_e$	η	-ω	$-\mu_e$	η	-ω	$-\mu_e$	η	-ω
$[Al(DFX)_2]^{3-}$	0.2606	0.1069	0.3176	0.2623	0.1074	0.3202	0.2623	0.1074	0.3203
$[Ga(DFX)_2]^{3-}$	0.2583	0.1063	0.3219	0.2595	0.1050	0.3206	0.2595	0.1049	0.3208
Al^{3+}	1.4403	2.2510	0.4608	1.4403	2.2510	0.4608	1.4403	2.2510	0.4608
Ga^{3+}	0.5055	0.3408	0.3749	0.5055	0.3408	0.3749	0.5055	0.3408	0.3749
DFX	0.2564	0.1106	0.2971	0.2584	0.1099	0.3038	0.2584	0.1099	0.3036

reactivity and a large band gap. Reasonably, the calculated band gaps (η) of the complexes are in a good agreement with the calculated equilibrium constants. In both complexes, the distribution of electron density is delocalized on the metallic center in the HOMO, while in the case of the LUMO state, the electron distribution is chiefly delocalized on the chelator molecules.

CONCLUSIONS

A comprehensive theoretical study was employed to investigate the deferasirox chelation potential in removing aluminum and gallium cations as the toxic metals. The optimized structures and equilibrium constants of the $[M(DFX)_2]^{3-}$ (M = Al, Ga) were calculated in the gas phase, water and DMSO, using B3LYP along with the relativistic Lanl2dz basis set for the metal centers. The highest value of the equilibrium constant belongs to $[Al(DFX)_2]^{3-}$ in the gas phase. To figure out the donor atom incorporation in the complex formation, NBO and QTAIM analyses were performed. The NBO analysis revealed that electron transfer from the $LP_{O,N}$ of the ligand into the aluminum LP* is less than that for gallium, confirming a more tendency of the DFX to chelate aluminum. DFT reactivity indices showed that $[Al(DFX)_2]^{3-}$ is a more stable complex than $[Ga(DFX)_2]^{3-}$. Moreover, it has less covalent character in comparison to the gallium complex. ELF and LOL studies confirmed the QTAIM results, verifying that both complexes have a partial covalent character, which is more for the gallium complexes. The TD-DFT study was carried out and the obtained results revealed that the solvent has a significant influence on the molecular orbital contribution in the absorption spectra of the studied complexes. For both complexes, λ_{max} has a greater value in the gas phase rather than similar analogous in the solvent. Consequently, based on our calculations, deferaisrox is considered as a good candidate for selective removing of aluminum and gallium, due to their stable complex formation in the biological systems.

ACKNOWLEDGEMENTS

Research council of Ferdowsi University of Mashhad is acknowledged for financial supports (Grant No. 3/28507).

REFERENCES

[1] Yu, Y.; Gutierrez, E.; Kovacevic, Z.; Saletta, F.; Obeidy, P.; Suryo Rahmanto, Y.; Richardson, R. D., Iron chelators for the treatment of cancer. *Curr. Med. Chem.* **2012**, *19*, 2689-2702. DOI: 10.2174/092986712800609706.

[2] Friedman, R., Drug resistance in cancer: molecular evolution and compensatory proliferation. *Onco. Target.* **2016**, *7*, 11746-11755. DOI: 10.18632/oncotarget.7459.

[3] Buetti-Dinh, A.; Pivkin, I.; Friedman, R., S100A4 and its role in metastasis-computational integration of data on biological networks. *Mol. Biosystems*. **2015**, *11*, 2238-2246. DOI: 10.1039/c5mb00110b.

[4] Rosengren, A. M.; Karlsson, B. C. G.; Nicholls, I., Monitoring of the distribution of warfarin in blood plasma. *ACS Med. Chem. Lett.* **2012**, *3*, 650-652. DOI: 10.1021/ml300112e.

[5] Chakravorty, D. K.; Li, P.; Tran, T. T.; Bayse, C. A.; Merz Jr, K. M., Metal ion capture mechanism of a copper metallochaperone. *Biochemistry* **2016**, *55*, 501-509. DOI: 10.1021/acs.biochem.5b01217.

[6] Aisen, P.; Iron in biochemistry and medicine II. In: Jacobs, A.; Worwood, M. (Eds.), New York, Academic Press, 1980, pp. 87-129.

[7] Exley, C., The toxicity of aluminium in humans. *Morphologie*. **2016**, *100*, 51-5. DOI: 10.1016/j.morpho.2015.12.003.

[8] Galanski, M.; Jakupec, M. A.; Keppler, B. K., Update of the preclinical situation of anticancer platinum complexes: novel design strategies and innovative analytical approaches. *Curr. Med. Chem.* **2005**, *12*, 2075-2094. DOI: 10.2174/0929867054637626.

[9] Woo, L. C. Y.; Yuen, V. G.; Thompson, K. H.; McNeill, J. H.; Orvig, C., Vanadyl-biguanide complexes as potential synergistic insulin mimics. *J. Inorg. Biochem.* **1999**, *76*, 251-257. DOI: 10.1016/S0162-0134(99)00152-X.

[10] Salehi, S.; Saljooghi, A. S.; Shiri, A., Synthesis, characterization and *in vitro* anticancer evaluations of two novel derivatives of deferasirox iron chelator. *Eur. J. Pharm*. **2016**, *781*, 209-217. DOI: 10.1016/j.ejphar.2016.04.026.

[11] Lebitasy, M.; Ampe, E.; Hecq, J. D.; Karmani, L.; Nick, H.; Galanti, L., Ability of deferasirox to bind iron during measurement of iron. *Clin. Chem. Lab. Med.* **2010**, *48*, 427-429. DOI: 10.1515/ CCLM.2010.080.

[12] Britton, R. S.; Leicester, K. L.; Bacon, B. R., Iron toxicity and chelation therapy. *Int. J. Hematol.* **2002**, *76*, 219-228. DOI: 10.1515/CCLM.2010.080.

[13] Goswami, D.; Machini, M. T.; Silvestre, D. M.; Nomura, C. S.; Esposito, B. P., Cell penetrating peptide (CPP)-conjugated desferrioxamine for enhanced neuroprotection: Synthesis and *in vitro* evaluation. *Bioconjugate Chem*. **2014**, *25*, 2067-2080. DOI: 10.1021/bc5004197.

[14] Loza-Rosas, S. A.; Vazquez-Salgado, A. M.; Rivero, K. I.; Negron, L. J., et al., Expanding the therapeutic potential of the iron chelator deferasirox in the development of aqueous stable Ti(IV) anticancer complexes. *Inorg. Chem.* **2017**, *56*, 7788-7802. DOI: 10.1021/acs.inorgchem.7b00542.

[15] Lauren, E. S.; Chris, O., Medicinal inorganic chemistry approaches to passivation and removal of aberrant metal ions in disease. *Chem. Rev.* **2009**, *109*, 4885-4910. DOI: 10.1021/cr9000176.

[16] Springer, S. D.; Butler, A., Microbial ligand coordination: Consideration of biological significance. *Coord. Chem. Rev*. **2015**, *306*, 628-635. DOI: 10.1016/ j.ccr.2015.03.013.

[17] Saljooghi, A. S.; Fatemi, S. J., Clinical evaluation of Deferasirox for removal of cadmium ionsin rat. *Biometals* **2010**, *23*, 707-712. DOI: 10.1007/s10534-010-9337-x.

[18] Saljooghi, A. S.; Fatemia, S. J., Removal of thallium by deferasirox in rats as biological model. *J. Appl. Toxicol.* **2011**, *31*, 139-143. DOI: 10.1002/jat.1573.

[19] Perl, D. P.; Brody, A. R., Alzheimer's disease: X-ray spectrometric evidence of aluminum accumulation in neurofibrillary tangle-bearing neurons. *Science* **1980**, *208*, 297-299. DOI: 10.1126/science.7367858.

[20] Kawahara, M. J., Effects of aluminum on the nervous system and its possible link with neurodegenerative diseases. *J. Alzheimers Dis.* **2005**, *8*, 171-185. DOI: 10.3233/JAD-2005-8210.

[21] Walton, J. R., Aluminum in hippocampal neurons from humans with Alzheimer's disease. *Neuro. Toxicol.* **2006**, *27*, 385-394. DOI: 10.1016/ j.neuro.2005.11.007.

[22] Lovell, M. A.; Ehmann, W. D.; Markesbery, W. R., Laser microprobe analysis of brain aluminum in Alzheimer's disease. *Ann. Neurol.* **1993**, *33*, 36-42. DOI: 10.1002/ana.410330107.

[23] Kasparkova, J.; Novakova, O.; Vrana, O.; Intini, F.; Natile, G.; Brabec, V., Molecular aspects of antitumor effects of a new platinum(IV) drug. *Mol. Pharmacol.* **2006**, *70*, 1708-1719. DOI: 10.1124/mol.106.027730.

[24] Lu, T.; Chen, F., Multiwfn: a multifunctional wavefunction analyzer. *J. Comput. Chem.* **2012**, *33*, 580-592. DOI: 10.1002/jcc.22885.

[25] Salehi, S.; Saljooghi, A. S.; Izadyar, M., Theoretical study on the electronic structures and equilibrium constants evaluation of Deferasirox iron complexes. *Comp. Biol. Chem.* **2016**, *64*, 99-106. DOI: 10.1016/ j.compbiolchem.2016.05.010.

[26] Frisch, J.; Trucks, G. W.; Schlegel, H. B.; Scuseria, G. E.; Robb, M. A.; Cheeseman, J. R.; Montgomery, J. A.; Vreven, T.; Kudin, K. N.; Burant, C. J.; *et al*., Gaussian 09; Gaussian, Inc.: Pittsburgh, P. A., 2009.

[27] Bartlett, R. J.; Purvis, G. D., Many-body perturbation theory, coupled-pair many-electron theory, and the importance of quadruple excitations for the correlation problem. *Int. J. Qua. Chem.* **1978**, *14*, 561-581. DOI: 10.1002/qua.560140504.

[28] Frey, P. A.; Reed, G. H., The ubiquity of iron. *ACS Chem. Biol.* **2012**, *7*, 1477-1481. DOI: 10.1021/ cb300323q.

[29] Reed, A. E.; Curtiss, L. A.; Weinhold, F., Intermolecular interactions from a natural bond orbital, donor-acceptor viewpoint. *Chem. Rev.* **1988**, *88*, 899-926. DOI: 10.1021/cb300323q.

[30] Kaviani, S.; Izadyar, M.; Housaindokht, M. R., Solvent and spin state effects on molecular structure, IR spectra, binding energies and quantum chemical reactivity indices of deferiprone-ferric complex: DFT study. *Polyhedron* **2016**, *117*, 623-627. DOI: 10.1016/ j.poly.2016.06.041.

[31] Chen, Z.; Wang, W.; Zhu, C.; Wang, L.; Fang, X.; Qiu; Y., Probing chemical bonding and optoelectronic properties of Square-Planar Aluminum, Gallium, and

nickel complexes. *Comput. Theor. Chem.* **2016**, *1090*, 129-133. DOI: 10.1016/j.poly.2016.06.041.

[32] Becke, A. D.; Edgecombe, K. E., A simple measure of electron localization in atomic and molecular systems. *J. Chem. Phys.* **1990**, *92*, 5397-5403. DOI: 10.1063/1.458517.

[33] Schmider, H. L.; Becke, A. D., Chemical content of the kinetic energy density. *J. Mol. Struct.* **2000**, *527*, 51-61. DOI: 10.1063/1.458517.

[34] Alajrin, M.; Marin-Luna, M.; Ortin, M. M.; Sanchenz-Andrada, P.; Vidal, A., Retro cheletropic ene reactions with 2-carbena-1,3-dioxolane as chelefuge. *Tetrahedron* **2011**, *67*, 5590-5595. DOI: 10.1016/j.tet.2011.05.119.

[35] Izadyar, M.; Gholizadeh, M.; Khavani, M.; Housaindokht, M. R., Quantum chemistry aspects of the solvent effects on 3,4-dimethyl-2,5-dihydrothiophen-1,1-dioxidepyrolysis reaction. *J. Phys. Chem. A* **2013**, *117*, 2427-2433. DOI: 10.1021/jp312746y.

[36] Martell, A. E.; Hancock, R. D., Metal Complexes in Aqueous Solutions, Plenum Press, New York, 1996.

[37] Pearson, R. G., Chemical Hardness, WILEY-VCH, New York, 1997.

[38] Popelier, P. L., Atoms in Molecules: An Introduction; Pearson Education: Harlow, U.K., 2000.

[39] Syzgantseva, O. A.; Tognetti, V.; Joubert, L., On the physical nature of halogen bonds: A QTAIM study. *J. Phys. Chem. A* **2013**, *117*, 8969-8980. DOI: 10.1021/jp4059774.

[40] Bader, R. F. W.; MacDougall, P. J.; Lau, C. D. H., Bonded and nonbonded charge concentrations and their relation to molecular geometry and reactivity. *J. Am. Chem. Soc.* **1984**, *106*, 1594. DOI: 10.1021/ja00318a009.

[41] Arabieh, M.; Platas-Iglesias, C., A density functional theory study on the interaction of dipicolinic acid with hydrated Fe^{2+} Cation. *Comput. Theor. Chem.* **2016**, *1090*, 134–146. DOI:10.1016/j.comptc.2016.06.010.

[42] Corral, I.; Gonzalez-Vazquez, J.; Martín, F., Potential energy surfaces of core-hole and shake-up states for dissociative ionization studies. *J. Chem. Theor. Comput.* **2017**, *13*, 1723-1736. DOI: 10.1021/acs.jctc.6b01214.

[43] Yang, W.; Mortier, W. J., The use of global and local molecular parameters for the analysis of the gas-phase basicity of amines. *J. Am. Chem. Soc.* **1986**, *108*, 5708-5711. DOI: 10.1021/ja00279a008.

[44] Xu, L.; Li, Q.; King, R. B., Unsaturated trinuclear iron fluoroborylene complexes. *J. Mol. Model.* **2017**, *23*, 123-132. DOI: 10.1007/s00894-017-3301-4.